Journal of
Mechanics of
Materials and Structures

NONLINEAR BENDING RESPONSE OF GIANT MAGNETOSTRICTIVE LAMINATED ACTUATORS IN MAGNETIC FIELDS

Yasuhide Shindo, Fumio Narita, Kotaro Mori and Tasuku Nakamura

Volume 4, Nº 5 May 2009

mathematical sciences publishers

JOURNAL OF MECHANICS OF MATERIALS AND STRUCTURES
Vol. 4, No. 5, 2009

NONLINEAR BENDING RESPONSE OF GIANT MAGNETOSTRICTIVE LAMINATED ACTUATORS IN MAGNETIC FIELDS

YASUHIDE SHINDO, FUMIO NARITA, KOTARO MORI AND TASUKU NAKAMURA

We report numerical and experimental investigations into the nonlinear bending behavior of magnetostrictive laminated actuators under magnetic fields. Magnetostrictive actuators were fabricated from thin layers of Terfenol-D and metal, and the magnetostriction of the devices was measured. A nonlinear finite element analysis was employed to evaluate the contribution of magnetic domain switching to the second-order magnetoelastic constants in the Terfenol-D layer. The effect of a magnetic field on the nonlinear deflection and internal stress of magnetostrictive laminated actuators is discussed.

1. Introduction

Smart materials, such as piezoelectric, magnetostrictive, and electrostrictive structures, are currently under intense investigation due to their ability to efficiently interconvert magnetic, electrical, and mechanical energies. Terfenol-D ($Tb_{0.3}Dy_{0.7}Fe_{1.9}$) is a highly magnetostrictive alloy of iron and the rare-earth metals [Moffett et al. 1991] terbium and dysprosium that stands out among smart materials in its ability to produce large actuation forces [Ryu et al. 2001]. An additional advantage of Terfenol-D over other smart materials is that it can be easily deposited onto nonmagnetic substrates. Recent work [Jia et al. 2006] has investigated applications of magnetostrictive materials as active actuators in layered bimorph structures. One limitation on the practical use of Terfenol-D is its nonlinear behavior [Wan et al. 2003]. Additionally, the tools available for modeling and design of magnetostrictive layered structures have not been sufficiently developed. To optimize the performance of magnetostrictive actuators, a detailed study into the nonlinear behavior of devices, especially under magnetic field driving, is necessary.

In this work, we report on the nonlinear bending behavior of magnetostrictive laminated actuators under magnetic fields in a combined numerical and experimental investigation. The fabricated magnetostrictive actuators consist of thin Terfenol-D and metal layers, and the magnetostriction of specimen devices was measured as a function of applied magnetic field strength. A nonlinear finite element analysis was also performed, and the contribution of magnetic domain switching to the second-order magnetoelastic constant in the Terfenol-D layer was evaluated. The effect of magnetic field strength on nonlinear deflection and internal stress for the magnetostrictive laminated actuators is examined.

Keywords: finite element method, material testing, giant magnetostrictive material, nonlinear bending.
This work was partially supported by the Grant-in-Aid for Exploratory Research from the Ministry of Education, Culture, Sports, Science and Technology, Japan.

2. Analysis

Basic equations. In the rectangular Cartesian coordinate system, x_1, x_2, x_3, the equations for magnetoelastic materials are

$$\begin{aligned} \sigma_{ji,j} &= 0, \qquad & H_i &= \phi_{,i}, \qquad & \varepsilon_{ij} &= s_{ijkl}\sigma_{kl} + d'_{kij}H_k, \\ B_{i,i} &= 0, \qquad & B_i &= d'_{ikl}\sigma_{kl} + \mu_{ik}H_k, \qquad & \varepsilon_{ij} &= \tfrac{1}{2}(u_{j,i} + u_{i,j}), \end{aligned}$$

where σ_{ij}, B_i, ε_{ij}, and H_i are the stress tensor, magnetic induction vector, strain tensor, and magnetic field intensity vector; u_i and ϕ are the displacement and magnetic potential; and s_{ijkl}, d'_{kij}, and μ_{ij} are the elastic compliance, magnetoelastic constant and magnetic permittivity. A comma followed by an index denotes partial differentiation with respect to the space coordinate x_i. We invoke the summation convention for repeated tensor indices. Valid symmetry conditions for the material constants are

$$s_{ijkl} = s_{jikl} = s_{ijlk} = s_{klij}, \qquad d'_{kij} = d'_{kji}, \qquad \mu_{ij} = \mu_{ji}.$$

For Terfenol-D, the constitutive relations can be written as

$$\begin{Bmatrix} \varepsilon_1 \\ \varepsilon_2 \\ \varepsilon_3 \\ \varepsilon_4 \\ \varepsilon_5 \\ \varepsilon_6 \end{Bmatrix} = \begin{bmatrix} s_{11} & s_{12} & s_{13} & 0 & 0 & 0 \\ s_{12} & s_{11} & s_{13} & 0 & 0 & 0 \\ s_{13} & s_{13} & s_{33} & 0 & 0 & 0 \\ 0 & 0 & 0 & s_{44} & 0 & 0 \\ 0 & 0 & 0 & 0 & s_{44} & 0 \\ 0 & 0 & 0 & 0 & 0 & s_{66} \end{bmatrix} \begin{Bmatrix} \sigma_1 \\ \sigma_2 \\ \sigma_3 \\ \sigma_4 \\ \sigma_5 \\ \sigma_6 \end{Bmatrix} + \begin{bmatrix} 0 & 0 & d'_{31} \\ 0 & 0 & d'_{31} \\ 0 & 0 & d'_{33} \\ 0 & d'_{15} & 0 \\ d'_{15} & 0 & 0 \\ 0 & 0 & 0 \end{bmatrix} \begin{Bmatrix} H_1 \\ H_2 \\ H_3 \end{Bmatrix},$$

$$\begin{Bmatrix} D_1 \\ D_2 \\ D_3 \end{Bmatrix} = \begin{bmatrix} 0 & 0 & 0 & 0 & d_{15} & 0 \\ 0 & 0 & 0 & d_{15} & 0 & 0 \\ d_{31} & d_{31} & d_{33} & 0 & 0 & 0 \end{bmatrix} \begin{Bmatrix} \sigma_1 \\ \sigma_2 \\ \sigma_3 \\ \sigma_4 \\ \sigma_5 \\ \sigma_6 \end{Bmatrix} + \begin{bmatrix} \mu_{11} & 0 & 0 \\ 0 & \mu_{11} & 0 \\ 0 & 0 & \mu_{33} \end{bmatrix} \begin{Bmatrix} H_1 \\ H_2 \\ H_3 \end{Bmatrix},$$

where

$$\begin{aligned} &\sigma_1 = \sigma_{11}, && \sigma_2 = \sigma_{22}, && \sigma_3 = \sigma_{33} \\ &\sigma_4 = \sigma_{23} = \sigma_{32}, && \sigma_5 = \sigma_{31} = \sigma_{13}, && \sigma_6 = \sigma_{12} = \sigma_{21}, \\ &\varepsilon_1 = \varepsilon_{11}, && \varepsilon_2 = \varepsilon_{22}, && \varepsilon_3 = \varepsilon_{33}, \\ &\varepsilon_4 = 2\varepsilon_{23} = 2\varepsilon_{32}, && \varepsilon_5 = 2\varepsilon_{31} = 2\varepsilon_{13}, && \varepsilon_6 = 2\varepsilon_{12} = 2\varepsilon_{21}, \\ &s_{11} = s_{1111} = s_{2222}, && s_{12} = s_{1122}, && s_{13} = s_{1133} = s_{2233}, \\ &s_{33} = s_{3333}, && s_{44} = 4s_{2323} = 4s_{3131}, && s_{66} = 4s_{1212} = 2(s_{11} - s_{12}), \\ &d'_{15} = 2d'_{131} = 2d'_{223}, && d'_{31} = d'_{311} = d'_{322}, && d'_{33} = d'_{333}. \end{aligned}$$

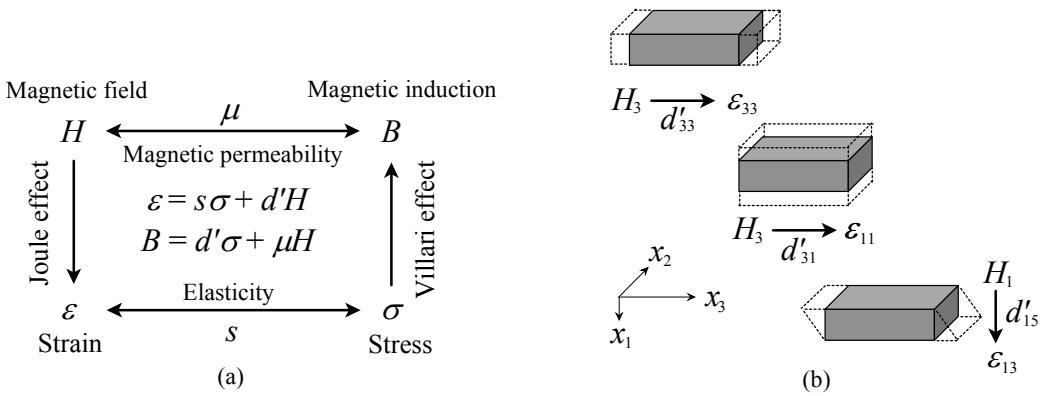

Figure 1. Magnetostrictive effect. (a) Mathematical relationships, (b) Various deformation modes.

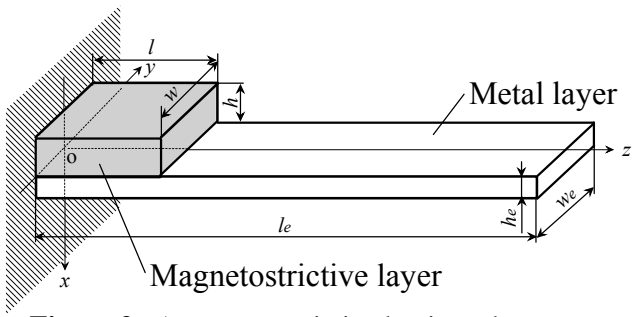

Figure 2. A magnetostrictive laminated actuator.

Figure 1(a) shows several physical effects related to the magnetostrictive effect [Yamamoto et al. 1999]. When a magnetic field is applied along the x_3-direction (easy axis) of the magnetostrictive material, both the longitudinal (33) and transverse (31) magnetostrictive deformation modes are excited, as shown in Figure 1(b). When a magnetic field is applied along the x_1-direction, the shear mode (15) is excited.

Finite element model. A magnetostrictive laminated plate is shown in Figure 2, in which a magnetostrictive layer of length l, width w, and thickness h is perfectly bonded on the top surface of a metal layer of length l_e, width $w_e = w$, and thickness h_e. The subscript e corresponds to the elastic layer. Dimensions $h(h_e)$, $w(w_e)$, and $l(l_e)$ are measured along the $x_1 = x, x_2 = y$, and $x_3 = z$ axis, respectively. The easy axis for magnetization of the magnetostrictive layer is the z-direction. The origin of the coordinate system is located at bottom left side of the magnetostrictive layer. The laminated plate is cantilevered, with $z = 0$ denoting the clamped end.

The laminated plate is subjected to a uniform magnetic field of magnetic induction $B_x = B_0$ or $B_z = B_0$. The constitutive relations of Terfenol-D layer are

$$\varepsilon_{xx} = s_{11}\sigma_{xx} + s_{12}\sigma_{yy} + s_{13}\sigma_{zz} + d'_{31}H_z, \qquad \varepsilon_{yz} = (s_{44}/2)\sigma_{yz} + (d'_{15}/2)H_y,$$
$$\varepsilon_{yy} = s_{12}\sigma_{xx} + s_{11}\sigma_{yy} + s_{13}\sigma_{zz} + d'_{31}H_z, \qquad \varepsilon_{zx} = (s_{44}/2)\sigma_{zx} + (d'_{15}/2)H_x,$$
$$\varepsilon_{zz} = s_{13}\sigma_{xx} + s_{13}\sigma_{yy} + s_{33}\sigma_{zz} + d'_{33}H_z, \qquad \varepsilon_{xy} = (s_{66}/2)\sigma_{xy},$$
$$B_x = d'_{15}\sigma_{zx} + \mu_{11}H_x, \qquad B_y = d'_{15}\sigma_{yz} + \mu_{11}H_y, \qquad B_z = d'_{31}\sigma_{xx} + d'_{31}\sigma_{yy} + d'_{33}\sigma_{zz} + \mu_{33}H_z.$$

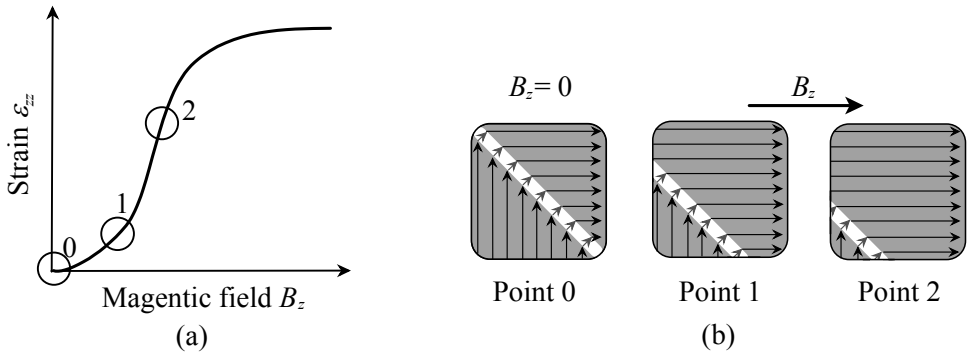

Figure 3. Schematic diagram of (a) strain versus magnetic field, and (b) domain structure.

Nonlinearity in the relationship between magnetostriction and magnetic field strength arises from movement of magnetic domain walls. The constants d'_{15}, d'_{31}, and d'_{33} for the Terfenol-D layer under $B_x = B_0$ become

$$d'_{15} = d_{15} + m_{15} H_x, \qquad d'_{31} = d_{31}, \qquad d'_{33} = d_{33}, \tag{1}$$

where d_{15}, d_{31}, d_{33} are the piezomagnetic constants and m_{15} is the second-order magnetoelastic constant. The constants d'_{15}, d'_{31}, and d'_{33} for the Terfenol-D layer under $B_z = B_0$ are

$$d'_{15} = d_{15}, \qquad d'_{31} = d_{31}, \qquad d'_{33} = d_{33} + m_{33} H_z, \tag{2}$$

where m_{33} is the second-order magnetoelastic constant. Figure 3 shows the relationship between magnetostriction (ε_{zz}) and magnetic field (B_z) strength along with the associated domain structure. A magnetic domain switching associated with 90° domain wall rotation gives rise to the nonlinear changes in magnetoelastic constants.

We performed finite element calculations to obtain the strain, deflection, and internal stresses for the magnetostrictive laminated plates. The equations describing magnetostrictive materials are mathematically equivalent to those describing piezoelectric materials [Tiersten 1969]. Therefore, coupled-field solid elements in ANSYS were used for the analysis. From (1) and (2) we see that the magnetoelastic constants d'_{15}, d'_{33} vary with the magnetic field due to domain wall movement. Making use of magnetic field-dependent material properties, the model calculated the nonlinear behavior.

Elastic stiffnesses ($\times 10^{-12}$m^2/N)					Piezo-magnetic constants ($\times 10^{-9}$m/A)			Magnetic permittivities ($\times 10^{-6}$H/m)	
s_{11}	s_{33}	s_{44}	s_{12}	s_{13}	d_{31}	d_{33}	d_{15}	μ_{11}	μ_{33}
17.9	17.9	26.3	−5.88	−5.88	−5.3	11	28	6.29	6.29

Table 1. Material properties of Terfenol-D.

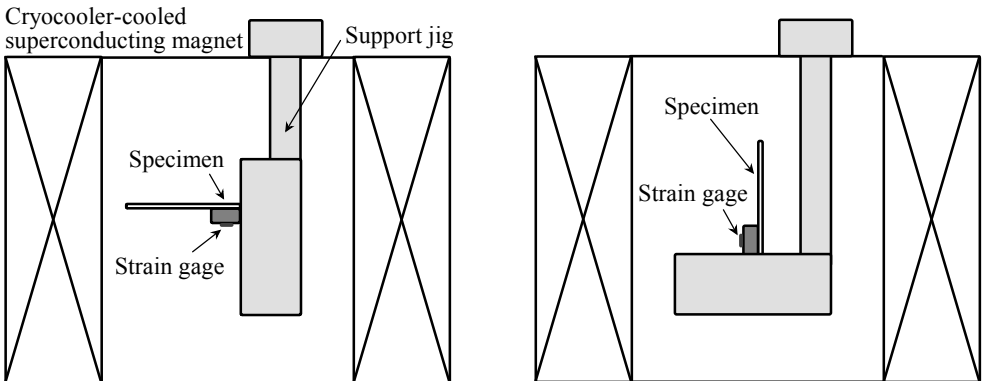

Figure 4. Experimental set-up of macroscopic strain measurement under magnetic fields normal (left) and parallel (right) to the easy axis. The magnetic field is in the vertical direction.

3. Experimental procedure

Magnetostrictive laminated actuators were prepared using Terfenol-D (ETREMA Products, Inc., USA) of $l = w = 10\,\text{mm}$ and SUS316 of $l_e = 40\,\text{mm}$, $w_e = 10\,\text{mm}$, and $h_e = 0.5\,\text{mm}$. The thickness of Terfenol-D was $h = 1, 3$, and $5\,\text{mm}$. Table 1 shows the material properties of Terfenol-D [Engdahl 2000; Nan et al. 2001]. The Young's modulus E and Poisson's ratio ν of SUS316 are $E = 189\,\text{GPa}$ and $\nu = 0.3$, respectively. We also consider the magnetostrictive laminated actuators (small size) using Terfenol-D of $l = w = 5\,\text{mm}$ and metal layer (SUS316, Cu or Al) of $l_e = 20\,\text{mm}$, $w_e = 5\,\text{mm}$, and $h_e = 0.5\,\text{mm}$. The thickness of Terfenol-D is $h = 0.5\,\text{mm}$. The Young's modulus E and Poisson's ratio ν of copper are $E = 130\,\text{GPa}$ and $\nu = 0.34$, while for aluminum they are $E = 70.3\,\text{GPa}$ and $\nu = 0.345$.

A strain gage was placed at the surface ($x = -h$, $y = 0$, $z = l/2$) of Terfenol-D. The magnetic field was then applied in the x- or z- direction, and the magnetostriction was evaluated. A cryocooler-cooled superconducting magnet with a 100 mm diameter working bore was used to create a static uniform magnetic field of magnetic induction B_0. A schematic diagram of the experimental set-up used to measure the macroscopic strain is shown in Figure 4. The magnetic field is applied vertically with respect to the apparatus orientation shown in the figure.

4. Results and discussion

We first present results for the magnetostrictive laminated actuators using Terfenol-D ($l = w = 10\,\text{mm}$) and SUS316 ($l_e = 40\,\text{mm}$, $w_e = 10\,\text{mm}$, $h_e = 0.5\,\text{mm}$). Figure 5 shows the strain ε_{zz} at $x = -1\,\text{mm}$, $y = 0\,\text{mm}$, and $z = 5\,\text{mm}$ versus applied magnetic field $B_z = B_0$ for the magnetostrictive laminated actuator with $h = 1\,\text{mm}$. Solid circles denote experimental data. The dashed line represents the values of strain predicted by the linear finite element analysis (FEA) and the solid line represents the strain after the second-order magnetoelastic constants have been considered. The constant $m_{33} = 1.4 \times 10^{-11}\,\text{m}^2/\text{A}^2$ is obtained, and agreement between nonlinear FEA and experiment is fair. Figure 6 shows similar results for the magnetostrictive laminated actuators with $h = 3$ and $5\,\text{mm}$, respectively. The constants m_{33} of

Terfenol-D layer with $h = 3$ and 5 mm are 4.4×10^{-12} and 1.1×10^{-12} m^2/A^2, respectively. The second-order magnetoelastic constant m_{33} decreases as the thickness of the magnetostrictive layers increases.

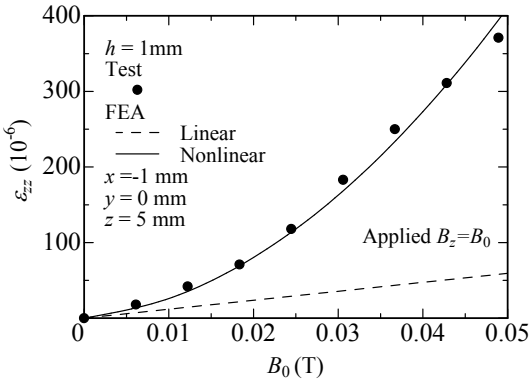

Figure 5. Strain versus magnetic field in the z-direction for $h = 1$ mm. Dashed line: values of strain predicted by the linear finite element analysis. Solid line: strain after second-order magnetoelastic constants have been considered.

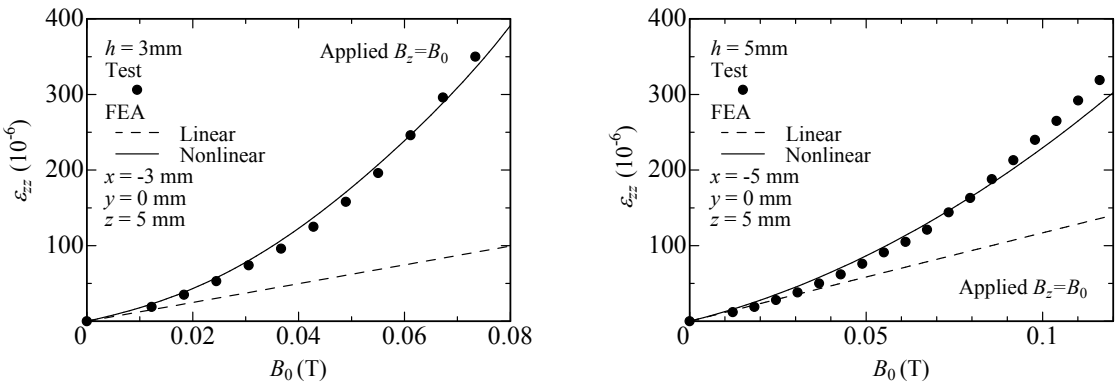

Figure 6. Strain versus magnetic field in the z-direction for $h = 3$ mm (left) and $h = 5$ mm (right).

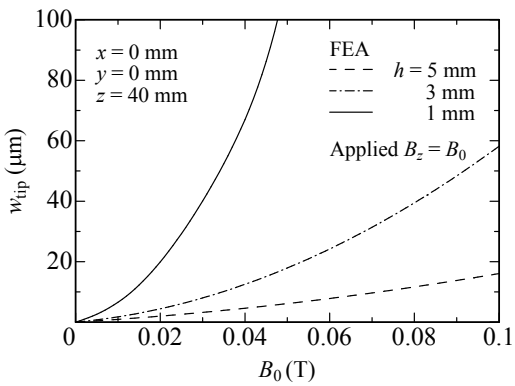

Figure 7. Tip deflection versus magnetic field in the z-direction for $h = 1$, 3, 5 mm.

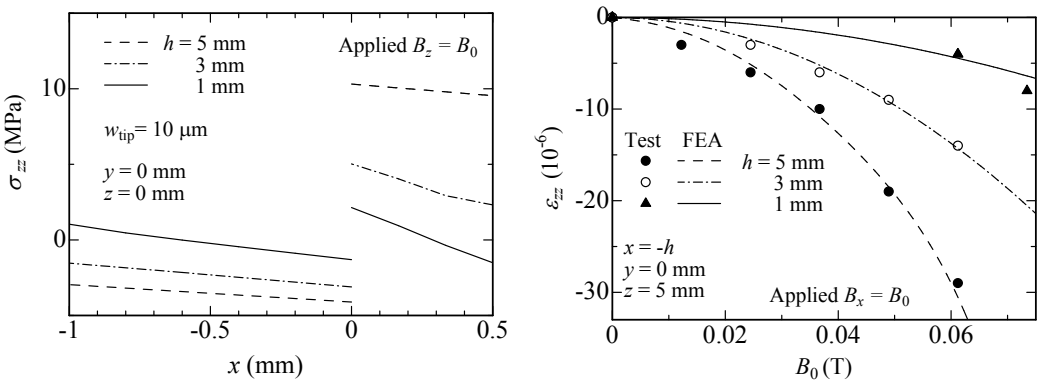

Figure 8. Left: normal stress distribution along the thickness direction at $y, z = 0$ for $h = 1, 3, 5$ mm. Right: Strain versus magnetic field in the x-direction for $h = 1,3,5$ mm.

Figure 7 shows the tip deflection w_{tip} at $x = 0$ mm, $y = 0$ mm, and $z = 40$ mm versus applied magnetic field $B_z = B_0$ for the magnetostrictive laminated actuators with $h = 1$, 3, and 5 mm. A nonlinear relationship between tip deflection and magnetic field is observed. The tip deflection increases as the thickness of the magnetostrictive layers decreases.

The variations of normal stress σ_{zz} along the thickness direction are calculated for the magnetostrictive laminated actuators at a chosen point ($y = 0$ mm and $z = 0$ mm here), and the results are shown in Figure 8, left. All calculations were done at a fixed tip deflection of 10 μm. The applied magnetic fields in the z-direction of the Terfenol-D layer under $w_{\text{tip}} = 10\,\mu$m are 0.074, 0.036, 0.014 T for $h = 5$, 3, 1 mm, respectively. Some stress gaps are present at the interface between Terfenol-D and SUS316 layers, as is expected. At smaller Terfenol-D thickness, lower normal stress is found for the same deflection. Also, a 10 μm deflection is produced at lower magnetic field.

Figure 8, right, shows strain ε_{zz} at $x = -h$ mm, $y = 0$ mm and $z = 5$ mm as a function of applied magnetic field $B_x = B_0$ for the magnetostrictive laminated actuators with $h = 1$, 3, 5 mm. The constants m_{15} of Terfenol-D layer with $h = 1$, 3, and 5 mm are 1.5×10^{-10}, 9.3×10^{-11}, and 3.7×10^{-11} m^2/A^2, respectively. The second-order magnetoelastic constant m_{15} decreases with an increase of the thickness of the magnetostrictive layers. By increasing the magnetostrictive layer thickness, the compressive strain of the Terfenol-D layer subjected to a magnetic field in the x-direction is raised. The tip deflection is also raised by increasing the thickness of the magnetostrictive layers (no figure shown), in contrast to the magnetostrictive laminated actuators subjected to a magnetic field in the z-direction. The tip deflection of the magnetostrictive laminated actuators under $B_z = B_0$ is much smaller than that under $B_x = B_0$.

Next, the bending behavior of the magnetostrictive laminated actuators (small size) using Terfenol-D ($l = w = 5$ mm, $h = 0.5$ mm) and a metal layer ($l_e = 20$ mm, $w_e = 5$ mm, $h_e = 0.5$ mm) is discussed. Figure 9, left, shows the plots of the strain ε_{zz} at $x = -0.5$ mm, $y = 0$ mm, and $z = 2.5$ mm against the applied magnetic field $B_z = B_0$ for the magnetostrictive laminated actuators of different elastic layers. Similar to the previous report [Jia et al. 2006], the second-order magnetoelastic constant depends on the elastic layers, and m_{33} of the Terfenol-D layer with SUS316, Cu, and Al are 9.9×10^{-12}, 1.7×10^{-11}, and 7.4×10^{-12} m^2/A^2, respectively. Figure 9, right, shows the corresponding tip deflection. The largest tip deflection is noted for the magnetostrictive laminated actuator with Cu. Figure 10 plots the variations

of normal stress σ_{xx} along the thickness direction at $y = 0$ mm and $z = 0$ mm for the magnetostrictive laminated actuators of different elastic layers under a fixed tip deflection of 10 μm. The applied magnetic fields in the z-direction of the Terfenol-D layer under $w_{\text{tip}} = 10\,\mu$m are 0.029, 0.022, 0.030 T for the actuators with SUS316, Cu, and Al, respectively. The stress gap under a constant tip deflection depends on the elastic layers.

5. Conclusions

Three-dimensional finite element analysis, in which the nonlinearity of Terfenol-D (the effect of magnetic domain switching) is incorporated into the model, is presented for magnetostrictive laminated actuators. The magnetostriction is also evaluated. We demonstrate that the mathematical procedure for this analysis is straightforward, and yields accurate values for the strain, as a function of magnetic field strength, present in the magnetostrictive laminated actuators. We find that the second-order magnetoelastic constants depend on the magnetostrictive layer thickness and elastic substrates, and that when a magnetic field is applied in the length direction, the tip deflection increases and the internal stress decreases with decreasing magnetostrictive layer thickness.

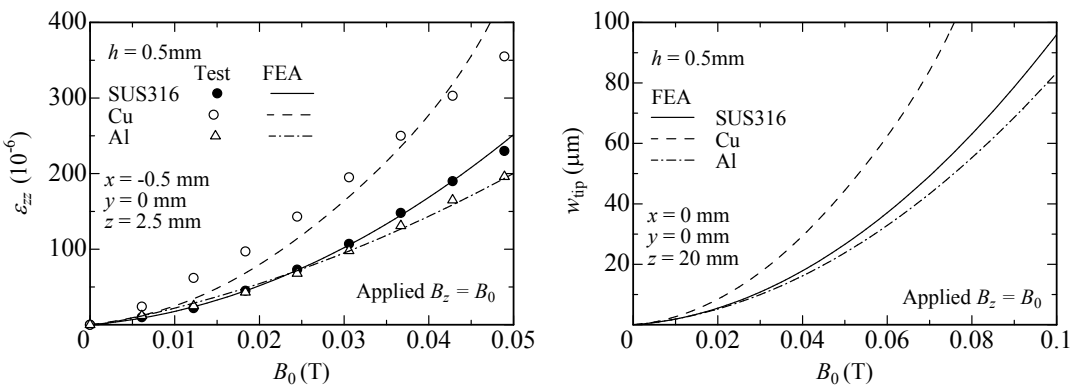

Figure 9. Strain (left) and tip deflection (right) versus magnetic field in the z-direction for different elastic layers.

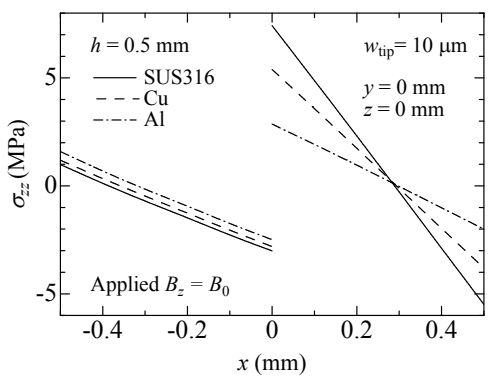

Figure 10. Normal stress distribution along the thickness direction at $y = 0$ and $z = 0$ mm for different elastic layers.

The present analysis can be applied to magnetostrictive laminated actuators with a wide range of magnetostrictive material and geometric properties. This study is also useful in designing magnetostrictive laminated devices and in reducing the problem of delamination that frequently occurs during service.

References

[Engdahl 2000] G. Engdahl (editor), *Handbook of giant magnetostrictive materials*, Academic Press, San Diego, CA, 2000.

[Jia et al. 2006] Z. Jia, W. Liu, Y. Zhang, F. Wang, and D. Guo, "A nonlinear magnetomechanical coupling model of giant magnetostrictive thin films at low magnetic fields", *Sens. Actuators A Phys.* **128**:1 (2006), 158–164.

[Moffett et al. 1991] M. B. Moffett, A. E. Clark, M. Wun-Fogle, J. Linberg, T. P. Teter, and E. A. McLaughlin, "Characterization of Terfenol-D for magnetostrictive transducers", *J. Acoust. Soc. Am.* **89**:3 (1991), 1448–1455.

[Nan et al. 2001] C. W. Nan, M. Li, and J. H. Huang, "Calculations of giant magnetoelectric effects in ferroic composites of rare-earth-iron alloys and ferroelectric polymers", *Phys. Rev. B* **63**:14 (2001), #144415.

[Ryu et al. 2001] J. Ryu, S. Priya, A. V. Carazo, K. Uchino, and H.-E. Kim, "Effect of the magnetostrictive layer on magnetoelectric properties in lead zirconate titanate/Terfenol-D laminate composites", *J. Am. Ceram. Soc.* **84**:12 (2001), 2905–2908.

[Tiersten 1969] H. F. Tiersten, *Linear piezoelectric plate vibrations: elements of the linear theory of piezoelectricity and the vibrations of piezoelectric plates*, Plenum, New York, 1969.

[Wan et al. 2003] Y. Wan, D. Fang, and K.-C. Hwang, "Non-linear constitutive relations for magnetostrictive materials", *Int. J. Non-Linear Mech.* **38**:7 (2003), 1053–1065.

[Yamamoto et al. 1999] Y. Yamamoto, H. Eda, and J. Shimizu, "Application of giant magnetostrictive materials to positioning actuators", pp. 215–220 in *1999 IEEE/ASME International Conference on Advanced Intelligent Mechatronics proceedings : AIM '99* (Atlanta, GA, 1999), IEEE, Piscataway, NJ, 1999.

Received 8 Apr 2008. Revised 2 Dec 2008. Accepted 17 May 2009.

YASUHIDE SHINDO: shindo@material.tohoku.ac.jp
Tohoku University, Department of Materials Processing, Graduate School of Engineering, Aoba-ku, Sendai 980-8579, Japan

FUMIO NARITA: narita@material.tohoku.ac.jp
Tohoku University, Department of Materials Processing, Graduate School of Engineering, Aoba-ku, Sendai 980-8579, Japan

KOTARO MORI: A8TM5628@stu.material.tohoku.ac.jp
Tohoku University, Department of Materials Processing, Graduate School of Engineering, Aoba-ku, Sendai 980-8579, Japan

TASUKU NAKAMURA: *Tohoku University, Department of Materials Processing, Graduate School of Engineering, Aoba-ku, Sendai 980-8579, Japan*